Algal Research 93 (2026) 104463

Contents lists available at ScienceDirect

Algal Research

journal homepage: www.elsevier.com/locate/algal

A new application of phycoerythrin and sulfated exopolysaccharides from *Porphyridium cruentum*: Effects on the regulation of lipid metabolism

Enrica Giustino [a], Paola Imbimbo [a], Jenifer Trepiana [b,c,d], Maria P. Portillo [b,c,d,*], Daria Maria Monti [a,*]

[a] Department of Chemical Sciences, University of Naples Federico II, via Cinthia 4, 80126, Naples, Italy
[b] Nutrition and Obesity Group, Department of Nutrition and Food Science, Faculty of Pharmacy and Lucio Lascaray Research Center, University of the Basque Country (UPV/EHU), 01006, Vitoria-Gasteiz, Spain
[c] CIBERobn Physiopathology of Obesity and Nutrition, Institute of Health Carlos III, 28222, Madrid, Spain
[d] BIOARABA Health Research Institute, 01006 Vitoria-Gasteiz, Spain

ARTICLE INFO

Keywords:
Oxidative stress
Microalgae
Biorefinery
Hepatic steatosis
Adipose tissue

ABSTRACT

Lipid-related disorders, including lipid accumulation into adipose tissue, obesity, insulin resistance, as well as fatty liver disease share oxidative stress as one of the key pathways involved. Antioxidant molecules obtained from natural sources can be used to encounter consumers' concerns about chemically synthesized ones. It is well established that microalgae are a reliable source of a wide variety of environmentally friendly and safe antioxidant molecules. In particular, *Porphyridium cruentum* has been studied as an abundant source of phycoerythrin and sulfated exopolysaccharides, both endowed with a potent antioxidant activity. Here, for the first time, phycoerythrin and sulfated exopolysaccharides were explored for their ability to interfere with 3T3-L1 adipocytes differentiation, affect *de novo* lipogenesis and enhance lipolysis in mature adipocytes, as well as to counteract lipid storage in AML12 hepatocytes, used as a hepatic steatosis model. The isolated antioxidant molecules affected pre-adipocytes differentiation inhibiting the master regulator of adipogenesis and genes involved in adipocyte maturation. In the hepatic steatosis model, sulfated exopolysaccharides were able to inhibit *de novo* lipogenesis whereas phycoerythrin showed a pro-fat effect. This study highlights that counteracting the oxidative stress is a necessary although not sufficient condition to counteract all lipid-related disorders.

1. Introduction

Oxidative stress is defined as an imbalance between reactive oxygen species (ROS) production and their clearance, resulting in cellular damage and metabolic alteration [1]. As highly reactive molecules, ROS can damage cellular macromolecules, altering their functions and promoting the insurgence of diseases of different nature and severity [2–4]. Oxidative stress, inflammation and obesity onset are strongly related [5], as oxidative stress can enhance pre-adipocyte proliferation, adipocyte differentiation and growth, as well as lipid storage in the liver [6]. Indeed, oxidative stress alters mitochondrial activity and inflammation mediators, both responsible for promoting lipogenesis and stimulating pre-adipocytes differentiation into mature adipocytes, responsible for the adipogenic processes [7,8]. The antioxidant pathways modulate also non-alcoholic fatty liver disease (NAFLD), a term referred to a wide range of chronic liver diseases, phenotypically indistinguishable from alcoholic hepatitis but that occurs independently from ethanol consumption [6,9–11]. Even if the real pathogenesis of NAFLD is still not identified, it is clear that the build-up of fat in the liver, as well as oxidative stress, play a crucial role in hepatic dysfunction. Currently, NAFLD treatments include diet, physical exercise, and medication, but no specific treatments have been found so far [12].

In this scenario, natural antioxidants could offer promising ways to prevent lipid metabolism-related diseases by mitigating oxidative stress and inflammation [13–15]. Microalgae are photosynthetic microorganisms, able to live in different environments, producing many bioactive molecules, such as polyunsaturated fatty acids (PUFAs), pigments (chlorophylls, carotenoids and phycobiliproteins), carbohydrates, and proteins. Many of these molecules show antioxidant, anticancer, antibacterial, antiviral, and antifungal activity [61]. In particular, a peculiar photosynthetic light-harvesting antenna complex, the phycobilisome, is present in *Cyanobacteria* (blue-green algae), *Rhodophyta* (red

* Corresponding authors.
E-mail addresses: mariapuy.portillo@ehu.eus (M.P. Portillo), mdmonti@unina.it (D.M. Monti).

https://doi.org/10.1016/j.algal.2025.104463
Received 3 July 2025; Received in revised form 10 October 2025; Accepted 3 December 2025
Available online 4 December 2025

algae), *Cryptophytes* and *Glaucophytes* [16,17]. The phycobilisome is composed by different phycobiliproteins, mainly represented by phycocyanin and phycoerythrin. Each phycobiliprotein is a chimera between a protein and a phycobilin [18]. Phycoerythrin (PE) in particular, is a high-value bioactive metabolite, largely used as a molecular marker thanks to its brilliant red color, but also in the cosmetics and food industry as a dye (*e.g.* for lipsticks, eyeliners, eye shadows, ice cream, candies) [19,20]. Phycoerythrin's ability to act as an anti-inflammatory molecule, as a preventive antioxidant agent, and to chelate metal ions responsible for the production of ROS, depicts it as the perfect candidate for therapeutic applications in oxidative stress-related diseases [21]. However, only few microalgae strains belonging to *Porphyridiophyaceae* class are able to synthesize high PE levels [22].

Besides PE, polysaccharides (PSs), represent up to 50 % of total algal biomass dry weight and serve as storage and/or structural compounds within algal cells [23]. In particular, sulfated polysaccharides (s-PSs) are well known for their primary antioxidant activity [24]. Given their structure and bioactivity, s-PSs may be used in the production of cosmetics, pharmaceuticals, and high-nutritional food additives. In particular, their antioxidant activity can be exploited for cosmetic or skin-care products as anti-aging and wrinkle-removing compounds [25]. It has been reported that PSs from microalgae, in particular from *Chlorella pyrenoidosa* and *Spirulina platensis*, are able to reduce fat accumulation by modulating fat deposition in the liver and epididymal white adipose tissues of obese mice [26]. Among microalgae, the red marine mesophile microalga *Porphyridium cruentum* is an interesting candidate for the extraction of high-value antioxidants. Indeed, *P. cruentum* is a well-known PE and sulfated exopolysaccharides (s-EPSs) producer, with the latter being released in the culture medium during cell growth.

In our previous papers, the set-up of *P. cruentum* cultivation and a biorefinery process for the extraction of proteins, s-EPSs, carotenoids and lipids has been reported, along with a deep chemical and biological characterization of PE and s-EPSs [27,28]. PE was isolated following a green approach to obtain the protein with an analytical purity grade ($\geq$ 4), which allowed to resolve its crystallographic structure [27]. s-EPSs, isolated from the exhausted culture medium, were chemically characterized by GC–MS chromatography which revealed the presence of xylose, galactose, glucose and by elemental analysis, which showed a 7 % of sulfur content, a value commonly found in s-EPSs biologically active [27]. Both molecules exerted a strong antioxidant activity on cell-based models, inhibiting ROS production, preventing GSH depletion and blocking lipid peroxidation [28]. Starting from the antioxidant activity of PE and s-EPSs, here, for the first time, these molecules were used to study their ability to counteract adipocytes differentiation, to affect lipid metabolism in mature 3T3-L1 adipocytes, as well as to prevent hepatic steatosis in AML12 cell-based model.

2. Materials and methods

2.1. Reagents

All reagents were purchased from Sigma-Aldrich (St. Louis, MO, USA), unless differently indicated.

2.2. Microalgae cultivation and bioactive molecules extraction

Porphyridium cruentum (CCALA 415) was purchased from the Culture Collection of Autotrophic Organism (CCALA, Centre for Phycology, Institute of Botany of the AS CR, Dukelská 135, TŘEBOŇ CZ-379 82, Czech Republic) and grown in closed systems with constant light (13 $\pm$ 1 PAR [($\mu mol_{photons}/m^2$)/s]) and temperature (25 $\pm$ 1 °C) as previously reported [27]. At the end of cell growth, *P. cruentum* culture was harvested by centrifugation (30 min, 1200 *g*, room temperature) to separate the culture medium from the wet biomass. Phycoerythrin (PE) was extracted from the wet biomass, whereas s-EPSs were recovered from the medium as previously reported [27]. Briefly, the equivalent of 200 mg dry weight biomass, were washed two times in double distilled H_2O, resuspended in 20 mL of PBS 50 mM pH 7.4, and sonicated for 20 min (30″ on, 30″ off) on ice at 40 % amplitude of the instrument (Bandelin Sonoplus HD 3200, MS73 tip). Then, Phycoerythrin was isolated by a single step size-exclusion chromatography, performed by using a Sephadex G-75 equilibrated in PBS 50 mM pH 7.4, and PE purity grade was measured using the Abs_{562nm}/Abs_{280nm} ratio. s-EPSs were isolated by ethanol precipitation (1:2 medium:ethanol *v/v*), recovered by centrifugation (12000 *g*, 30 min, 4 °C), and lyophilized.

2.3. Cell culture and biocompatibility evaluation

Murine pre-adipocytes (3T3-L1) and mouse hepatocyte (AML12) cell lines were purchased from ATCC (Manassas, VA, USA). 3T3-L1 were cultured in Dulbecco's modified Eagle's medium (DMEM) (GIBCO, BRL Life Technologies, Grand Island, NY), supplemented with 10 % fetal bovine serum, 2 mM L-glutamine, and antibiotics, whereas AML12 were grown in DMEM/HAM's F12 Glutamax (GIBCO, BRL Life Technologies, Grand Island, NY) medium supplemented with 10 % fetal bovine serum, 5 μg/mL transferrin, 5 ng/mL selenium, 5 μg/mL insulin, 40 ng/mL dexamethasone and antibiotics. Both cell lines were cultured at 37 °C in a 5 % CO_2 humidified atmosphere. The biocompatibility of PE and s-EPSs on 3T3-L1 was evaluated by the MTT assay. Cells were seeded in a 96-well plate at a density of 3 $\times$ 10^3 cell/well and incubated with increasing concentrations of s-EPSs (0.5–50 μg/mL) and PE (0.01–20 nM). After 24 and 48 h incubation, cell viability was assessed by the MTT assay [29]. Cell survival was expressed as the percentage of viable cells in the presence of the molecules compared to control cells (*i.e.*, cells grown in DMEM in the absence of any molecule).

2.4. Experimental cell system

3T3-L1 preadipocytes were differentiated into their adipocyte phenotype as previously reported [30] and incubated with different concentrations of PE or s-EPSs at every step of differentiation, until day 8. As for the AML12, cells were seeded in 6-well plates at 2 $\times$ 10^5 cells/well concentration and incubated with Palmitic Acid (PA) to induce triglyceride accumulation mimicking an *in vitro* steatosis model as reported by González-Arceo and colleagues [31]. After 72 h from seeding, cells were incubated with 0.3 mM PA for 18 h in the presence or absence of the molecules. For both cell lines, PE was tested at 5 and 10 nM, whereas s-EPSs were added at 5, 10, and 12 μg/mL. Images of cells before and after treatment were acquired by an Olympus CH optical microscope (Olympus, Tokyo, Japan) at 10× magnification. At the end of the experiments, cells were harvested and lysed to analyze triglyceride accumulation, mRNAs and proteins expression.

2.5. Effect of PE and s-EPSs on 3T3-L1 mature adipocytes

To analyze the effect of *P. cruentum* PE and s-EPSs on mature adipocytes, 3T3-L1 cells were differentiated as reported above until day 12 and then treated for 24 h with either PE (5 and 10 nM) or s-EPSs (5, 10, 12 μg/mL). At the end of the treatment, cells were extensively washed with 0.01 M PBS pH 7.4 to measure triglyceride accumulation and analyze mRNAs and proteins expression.

2.6. Triglyceride and protein content evaluation

Total triglycerides (TG) content was measured spectrophotometrically by using a commercial kit (Spinreact, Girona, Spain), as previously reported [32]. Briefly, cells were harvested by adding 150 μL/well of lysis buffer (0.01 M Tris-HCl pH 7.4, 0.15 M NaCl, 1 mM EDTA) supplemented with protease inhibitors and sonicated for 5 s continuously at 40 % of the instrument amplitude (Branson Digital Sonifier SFX 550). Total TG content were measured and reported as the percentage of the ratio between mg of TG and mg of total protein, measured by the

Bradford assay [33], with respect to control cells, *i.e.*, cells differentiated in the absence of molecules.

2.7. Western blot analyses

Proteins expression levels were measured by Western Blot analyses. At the end of treatments, cells were harvested by adding 150 μL/well of RIPA buffer, supplemented with proteases and phosphatases inhibitors, and lysed by incubating samples on ice for 30 min, vortexing every 5 min. Proteins were recovered in the supernatant by centrifugation at 14000 *g* for 15 min at 4 °C and quantified by the BCA assay (Thermo-Fisher, Waltham, MA, USA) [34]. 30 μg of proteins were separated by SDS-PAGE in 4–15 % polyacrylamide gradient gels and electroblotted on polyvinylidene difluoride (PVDF) membranes by constant amperage (1 mA/cm^2). Membranes were blocked for 1 h with 4 % BSA at room temperature and then incubated with specific antibodies: anti-CCAAT Enhancer Binding Protein Beta (c/EBPβ, Cell Signaling, Danvers, MA, USA, #3087, rabbit), anti-Peroxisome Proliferator-Activated Receptor gamma (PPARγ, Cell Signaling, #2430, rabbit), anti-Adiponectin (Cell Signaling, #2789, C4B-10, rabbit), anti-phospho-Acetyl-CoA Carboxylase (pACC, Cell Signaling, #3661, rabbit), anti-Acetyl-CoA Carboxylase (ACC, Cell Signaling, #4190, rabbit), anti-phospho-Hormone Sensitive Lipase (pHSL, Cell Signaling, #4126, rabbit), anti-Hormone Sensitive Lipase (HSL, Cell Signaling, #4107, rabbit), anti-Fatty Acid Synthase (FAS, Abcam, ab128870, rabbit), anti-Adipose Triglyceride Lipase (ATGL, Cell Signaling, #2138, rabbit) and anti-β-actin (Sigma-Aldrich, A5441, mouse). Band detection and densitometric analyses were performed using a ChemiDoc (Biorad, Hercules, CA, USA), according to the manufacturer's instruction.

2.8. RNA extraction and qRT-PCR

The effect of s-EPSs and PE on the genes related to preadipocyte differentiation pathway and lipid metabolism was analyzed by quantitative Real-Time Polymerase Chain Reaction (qRT-PCR) on the purified and retro-transcribed mRNA extracted from 3T3-L1 at day 8 and day 13, as previously reported [35]. Relative *Cebpβ*, *Srebf1*, *Pparγ*, *Adiponectin*, *Glut4*, *Acc*, *Hsl*, *Fas* and *Atgl* mRNA levels were measured by Real-Time PCR (RT-PCR) (CFX96 Real-Time System) at 60 °C by adding 4.75 μL of each cDNA to a mixture of 5 mM of forward and reversed primers, and SYBR Green Master Mix (Applied Biosystems). β-actin was used as housekeeping gene. Results are expressed as fold changes in threshold cycle (Ct) values compared to the controls using the $2^{-\Delta\Delta Ct}$ method [36]. Specific commercially synthesized primers sequences are reported in Table 1.

Table 1
Primer sequences for real-time PCR genes.

Gene	Forward primer	Reverse primer
Cebpβ	5'-CAAGCTGAGCGAGTCCA-3′	5'-CAGCTGCTCCACCTTCTTCT-3′
Srebf1	5'-GTCGTTGGCATCCTGCTATC-3′	5'-TAGCTGGAAGTGACGGTGGT-3′
Pparγ	5'-TCGCTGATGCACTGCCTATG-3′	5'-GAGAGGTCCACAGAGCTG-3′
Adiponectin	5'-GACGACACCAAAAGGGTCCA-3'	5'-GAGTGCCATCTCTGCCA-3'
Atgl	5'-GAGCTTCGCGTCACCAAC-3'	5'-CACATCTCTCGGAGGACC-3'
Glut4	5'-GTCCTCACAGTACTCCCTGC-3'	5'-AGGTATCTGGGGCTCTCAGG-3'
Acc	5'-GGAGCCAGAAGGGACAGTAG-3'	5'-CAGCCAAGCGGATGTAAACT-3'
Hsl	5′- AGCCCCTCAAGTGCACAGTG-3'	5′- TGCCAATGTGTTTTCCCTGA-3'
Fas	5'-AGCCCCTCAAGTGCACAGT-3'	5'-TGCCAATGTGTTTTCCCTG-3'
β-actin	5'-CCCGCGAGTAGAACCTTCT-3'	5'-CGTCATCCATGGCGAACT-3'

Cebpβ: CCAAT Enhancer Binding Protein Beta; *Srebf1*: Sterol Regulatory Element-Binding Factor 1; *Pparγ*: Peroxisome Proliferator-Activated Receptor gamma; *Atgl*: Adipose Trygliceride Lipase; *Glut4*: Glucose Transporter Type 4; *Acc*: Acetyl-CoA Carboxylase; *Hsl*: Hormone Sensitive Lipase; *Fas*: Fatty Acid Synthase.

2.9. Statistical analyses

Results are reported as mean of three independent experiments (mean ± S.D.) and compared through one-way analysis of variance (ANOVA) according to Bonferroni's method (*post hoc*), using GraphPad Prism for Windows, version 6.01. For cell viability, triglyceride-lowering effects, gene and protein expressions, each concentration tested was compared to control cells. No comparison among cell groups was carried out. In the case of hepatocytes, each treated group was compared either to control hepatocytes or hepatocytes incubated with Palmitic Acid alone. Statistical significance was set at $p \leq 0.05$.

3. Results

3.1. Porphyridium cruentum cultivation, s-EPSs isolation and phycoerythrin purification

Porphyridium cruentum was cultivated in column photobioreactors with a specific growth rate of 0.2 d^{-1}, reaching a maximum biomass concentration of 0.5 g/L D.W. At the end of the exponential phase, the culture was harvested by centrifugation to separate the s-EPSs-enriched exhausted medium from algae biomass. The biomass yield was 0.63 ± 0.05 g/L. s-EPSs were isolated by ethanol precipitation (1:2 *v/v*) from 800 mL of exhausted medium, with a final yield of 300 ± 67 mg/L. In a previous publication [27], the monosaccharide composition of s-EPSs fraction was reported and xylose, galactose, glucose, and traces of rhamnose, glucuronic acid, and glucosamine were found. Additionally, an elemental analysis was carried out to reveal the presence of 7 % sulfur content [27]. Finally, the Bradford assay revealed negligible amount of proteins (data not shown). In the same paper, PE was isolated from the aqueous extract, starting from the equivalent of 200 mg D.W. biomass. After ultrasound assisted extraction, 35 ± 4 % of total proteins were recovered, with 3.0 ± 0.4 % related to PE content [27]. Then, PE was purified by a size exclusion chromatography, achieving a purity grade of 4 (A_{565nm}/A_{280nm}), consistent with analytical-grade standards [37].

3.2. s-EPSs and PE biocompatibility on 3T3-L1 pre-adipocyte

As the evaluation of any possible toxic effect of bioactive molecules is a mandatory step for their commercial use in cosmeceutical or in pharmaceutical industries, the biocompatibility of s-EPSs and PE was evaluated on 3T3-L1 pre-adipocytes. Cell viability was measured by the MTT assay, as described in Material and Methods section. As reported in Fig. 1a, s-EPSs exerted a slight toxicity at high concentrations (25 μg/mL), whereas PE was found to be fully biocompatible at any experimental condition analyzed (Fig. 1b). Based on these results, and considering the concentration previously established as antioxidant (10 μg/mL for s-EPSs and 10 nM for PE, [27]), the range of concentration used for further analyses was between 0.5 and 12 μg/mL for s-EPSs and 0.5 and 10 nM for PE.

3.3. Effect of s-EPSs and PE on triglyceride accumulation in 3T3-L1 pre-adipocytes maturation

Given the above-mentioned correlation with oxidative stress, s-EPSs and PE from *P. cruentum* were tested for their ability to inhibit 3 T3-L1 pre-adipocyte differentiation. Total intracellular TG content was measured on cells after 8 days treatment with increasing concentrations of both molecules. The results are reported in Fig. 2, where the

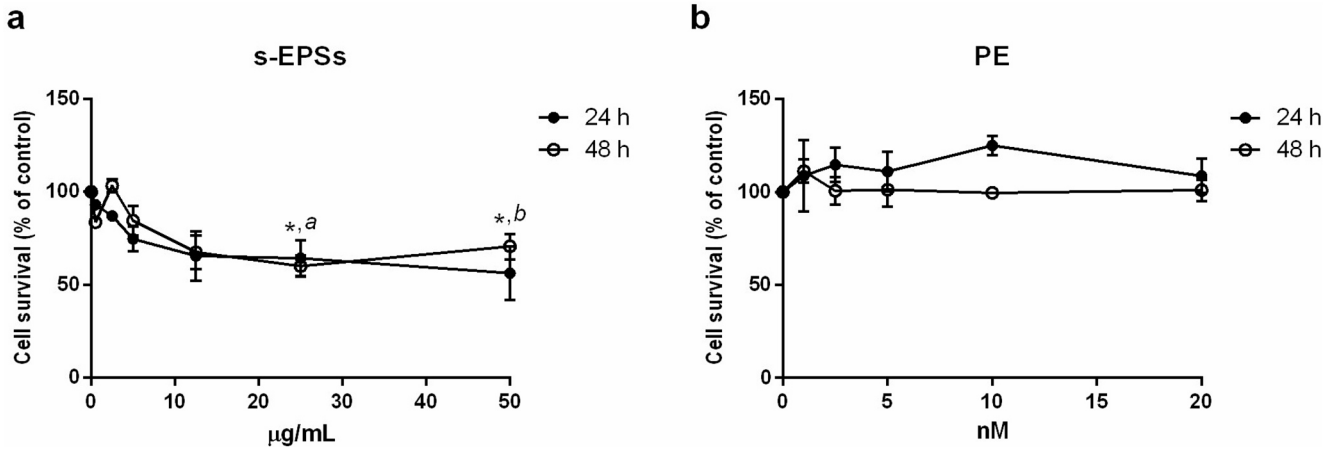

Fig. 1. Effects of s-EPSs and PE from *P. cruentum* on 3T3-L1 cell viability. Dose-response and time-dependent curves of 3 T3-L1 cells after 24 h (black circles) and 48 h (empty circles) incubation with increasing concentration of s-EPSs (0.5–50 μg/mL) (**a**) and PE (0.01–20 nM) (**b**). Cell viability was evaluated by the MTT assay and cell survival was expressed as percentage of viable cells in the presence of bioactive molecules, with respect to control cells grown in the absence of the molecules. * indicates $p < 0.05$ with respect to control cells upon 24 h incubation; *a* indicates $p < 0.05$, *b* indicates $p < 0.01$ with respect to control cells upon 48 h incubation.

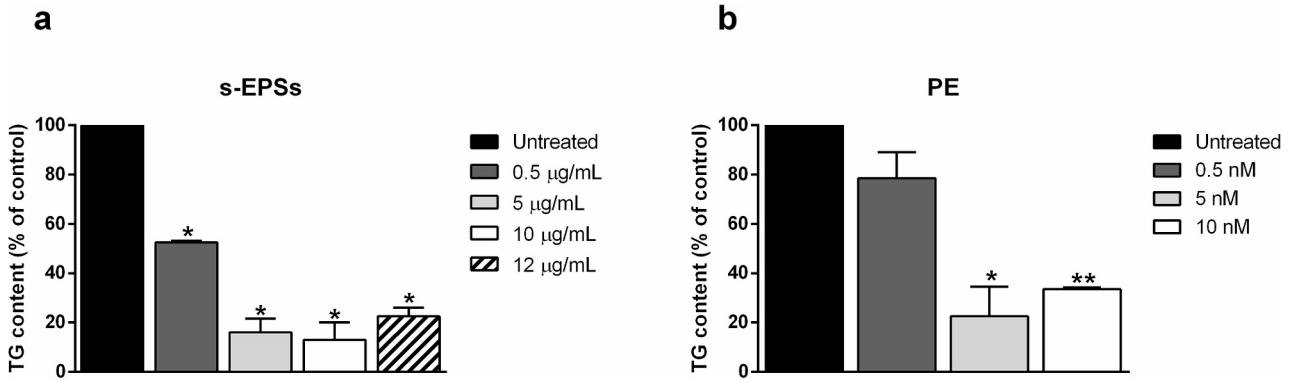

Fig. 2. 3T3-L1 pre-adipocyte triglyceride (TG) content after differentiation. Triglyceride accumulation was measured in 3T3-L1 preadipocytes after 8 days of differentiation in the presence or absence of s-EPSs and PE. (**a**) TG content upon incubation with different s-EPSs concentration: 0.5 μg/mL, dark grey bars; 5 μg/mL, light grey bars; 10 μg/mL, white bars and 12 μg/mL, dashed bars. (**b**) TG content upon incubation with different PE concentrations: 0.5 nM of PE, dark grey bars; 5 nM, light grey bars and 10 nM, white bars. Data are reported as the percentage of TG content with respect to cells differentiated in the absence of molecules (black bars), normalized to the total protein content. Results are reported as means ± S.D. of three independent experiments. * Indicates $p < 0.05$, ** $p < 0.005$, with respect to control cells.

percentage of the ratio between TG (mg) and total proteins (mg) with respect to the ratio obtained for control cells (*i.e.*, cells differentiated in the absence of antioxidants) is showed for each experimental condition. Interestingly, s-EPSs were able to significantly inhibit TG accumulation, from about 50 % at 0.5 μg/mL, up to almost 90 % at 10 μg/mL. PE was active from 5 nM (about 70 % inhibition).

3.4. Effects of s-EPSs and PE on the expression of protein involved in 3T3-L1 pre-adipocytes maturation

The genes involved in different phases of the adipogenic process were then analyzed: (i) c/EBPβ, a protein involved in the beginning of the transcriptional cascade which can activate the expression of (ii) PPARγ, the master regulator of adipogenesis, whose activation initiates the progression of cells into a mature adipocyte phenotype, *via* the activation of specific genes related to maturation, such as (iii) adiponectin and ATGL [38]. Considering the lowest concentration able to inhibit TG accumulation, the concentrations selected to investigate the mechanism of action exerted by s-EPSs and PE were 5 μg/mL and 5 nM, respectively. As shown in Fig. 3, both molecules were able to significantly affect the expression of the proteins analyzed, at different extent: s-EPSs induced about 40 % inhibition of c/EBPβ expression, whereas PE showed 70 % inhibition. Conversely, s-EPSs exerted 80 % inhibition of PPARγ expression, whereas PE 60 %. In the case of adiponectin, both molecules were able to inhibit its expression almost completely (about 90 %).

3.5. Effects of s-EPSs and PE on the expression of genes involved in 3T3-L1 pre-adipocytes maturation

qRT-PCR analyses were performed on three key proteins identified by Western Blot with two additional markers: (i) *Srebf1,* which encodes for the Sterol Regulatory Element-Binding Protein 1 (SREBP-1c), primarily found in adipose tissues, where it plays a crucial role in regulating lipid metabolism proteins by specifically up-regulating PPARγ expression, thus driving adipocyte differentiation; (ii) ATGL, a specific lipase synthetized by mature adipocytes, whose expression is related to adipocyte differentiation. Results are presented in Fig. 4, in which relative mRNA levels, normalized to *β-actin* levels, are reported. s-EPSs significantly inhibited the transcription of all the analyzed genes, suggesting that s-EPSs act on c/EBPβ, PPARγ and adiponectin at a transcriptional level. PE induced a slight but significant inhibition of *Cebpβ*

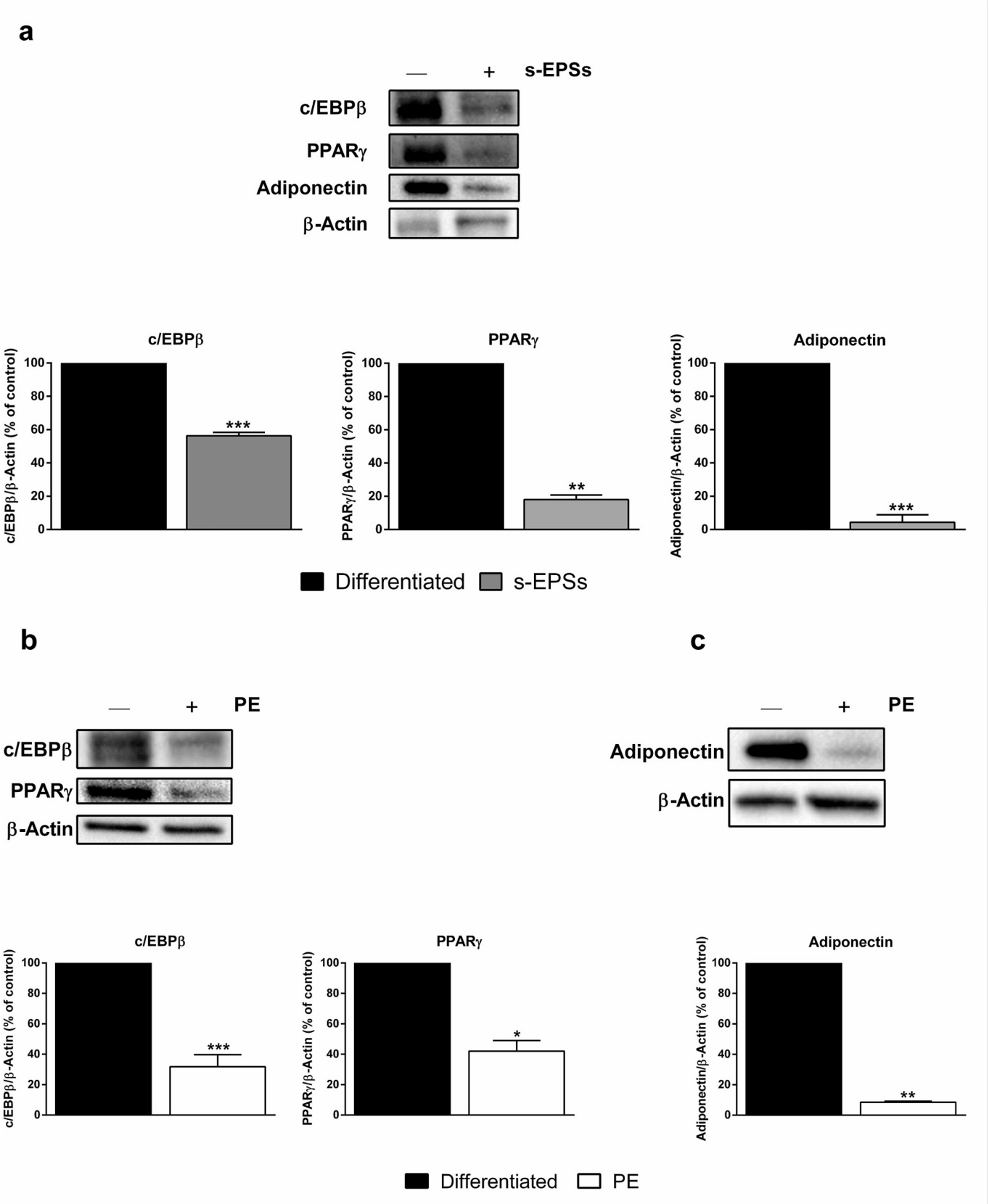

Fig. 3. Effect of s-EPSs and PE on c/EBPβ, PPARγ and adiponectin protein expression in 3T3-L1 pre-adipocytes. Cells were differentiated for 8 days as reported in Material and Methods section in the presence of 5 μg/mL s-EPSs (**a**) and 5 nM PE (**b, c**) added during all the differentiation steps. Cells were analyzed by Western Blot, using specific antibodies against c/EBPβ, PPARγ and adiponectin. β-actin was used as housekeeping protein. The relative densitometric analysis of c/EBPβ, PPARγ and adiponectin is reported in the histograms. Black bars refer to cells differentiated in the absence of any treatment and used as control. Data shown are the means ± S.D. of three independent experiments. * Indicates $p < 0.05$, ** indicates $p < 0.005$, *** $p < 0.001$, with respect to control cells.

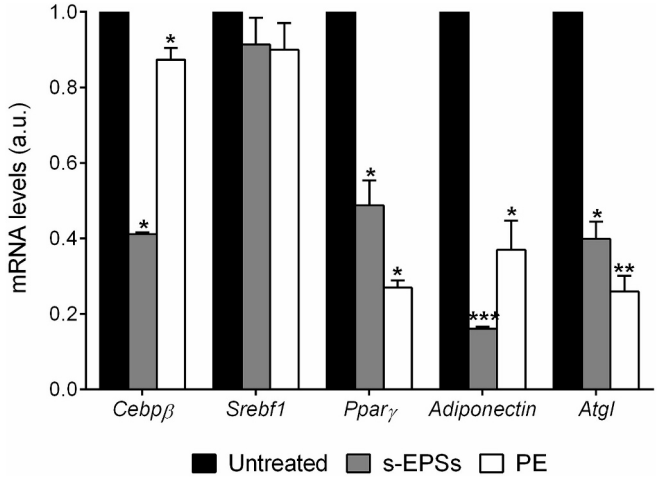

Fig. 4. Effects of s-EPSs and PE from *P. cruentum* on pre-adipocyte maturation gene expression. Relative mRNA levels of *C/ebpβ*, *Srebf-1*, *Pparγ*, *Adiponectin* and *Atgl* in 3T3-L1 cells differentiated for 8 days in the presence or absence of 5 μg/mL of s-EPSs (grey bars) or 5 nM of PE (white bars). Results are expressed as fold changes in threshold cycle (Ct) values compared to controls (black bars) using the $2^{-\Delta\Delta Ct}$ method. Data shown are means ± S.D. of three independent experiments. * Indicates $p < 0.05$, ** indicates $p < 0.005$, *** $p < 0.001$ with respect to cells differentiated in absence of any bioactive molecule.

(about 20 %), sufficient to inhibit the whole transcriptional cascade, confirmed by a significant inhibition of *Pparγ, Adiponectin* and *Atgl* expression at a transcriptional level. Neither s-EPSs or PE were able to inhibit the expression of *Srebf1*.

3.6. Effects of s-EPSs and PE on 3T3-L1 mature adipocytes

In light of the interesting results obtained on adipocytes differentiation, the effect of s-EPSs and PE on mature adipocytes was investigated by measuring TG content after 24 h incubation with each molecule. A significant reduction (about 30 %) was observed when cells were treated with the highest concentration of s-EPSs (Fig. 5), but no significant reduction was observed upon PE incubation. Thus, 12 μg/mL s-EPSs was chosen for Western Blot and qRT-PCR analyses. PE was further used at 10 nM, the concentration endowed with antioxidant activity [28].

Changes in genes and proteins involved in the *de novo* lipogenesis (Acetyl-CoA Carboxylase, *Acc* and Fatty Acid Synthase, *Fas*) were analyzed in mature adipocytes, upon incubation with either s-EPSs or PE. FAS is known to be involved in the first steps of fatty acid synthesis, whereas ACC is involved in the upstream process, as it catalyzes the conversion of Acetyl-CoA in Malonyl-CoA [39]. The ratio pACC/ACC was measured, as ACC is inactivated upon phosphorylation. In the case of s-EPSs, Western Blotting and qRT-PCR analyses did not show any significant alteration in ACC or FAS levels, with respect to untreated cells (Fig. 6a, Fig. 6b and Fig. 7, grey bars). PE exerted a significant inhibition only in *Fas* gene expression (Fig. 7), but this effect was not confirmed at protein level (Fig. 6b, white bars), meaning that *de novo* lipogenesis was not affected.

For the lipolytic pathway, two enzymes involved in triglycerides breakdown were analyzed: Hormone-Sensitive Lipase (*Hsl*) and Adipose Triglyceride Lipase (*Atgl*), as well as the Glucose transporter (*Glut4*), the main transporter responsible for glucose uptake. During lipolysis, ATGL catalyzes TG hydrolyses into diglycerides (DGs), which are then degraded into monoglycerides by phosphorylated HSL [40]. Upon treatment with s-EPSs, ATGL protein expression significantly decreased compared to untreated cells (Fig. 6c, grey bar), whereas no changes in the pHSL/HSL protein expression was observed (Fig. 6d, grey bar). This regulation is only related to protein expression, as no changes in *Atgl* and *Hsl* gene expression were observed (Fig. 7). Different results were obtained with PE, able to increase pHSL/HSL ratio (Fig. 6d, white bar), indicative of an activation of the last step of the lipolytic pathway. Accordingly, also the *Hsl* gene expression was significantly increased (Fig. 7). However, neither ATGL protein or mRNA were affected upon incubation with PE (Fig. 6c, white bar and Fig. 7).

3.7. Effect of s-EPSs and PE on a hepatic steatotic model system

Finally, s-EPSs and PE were tested for their potential ability to counteract lipid accumulation in AML12 cells, a hepatic steatosis cell model. Thus, lipid accumulation was induced by palmitic acid (PA) and the experimental system set-up was verified by measuring TG content, lipolysis pathway (ATGL and pHSL/HSL ratio) and markers of *de novo* lipogenesis (pACC/ACC ratio and FAS) (Fig. 8). Globally, when cells were incubated with PA, a significant increase in TG content was measured (Fig. 8a), suggesting a successful steatosis induction. Western blot analyses revealed a significant decrease in the pACC/ACC levels in cells treated with PA (Fig. 8b, grey bars), thus suggesting the activation of the *de novo* lipogenesis, as well as a significant decrease in the pHSL/HSL ratio (Fig. 8e), indicating the inhibition of the lipolytic pathway. However, the lipid accumulation after PA treatment was not supported by FAS upregulation (Fig. 8c). This result could be ascribed either to high intracellular fatty acid consumption, so that TG content increases bypassing FAS activity, or to a negative regulation of the enzyme [41]. These hypotheses are supported by some evidence: FASN knockout in liver promoted hepatic steatosis in mice on a zero-fat diet [42,43]; in NAFLD state, the increased FAs intake induces a significant increase in their mitochondrial oxidation for a compensatory adaptation mechanism. This results in an increase in oxidative stress and inflammation,

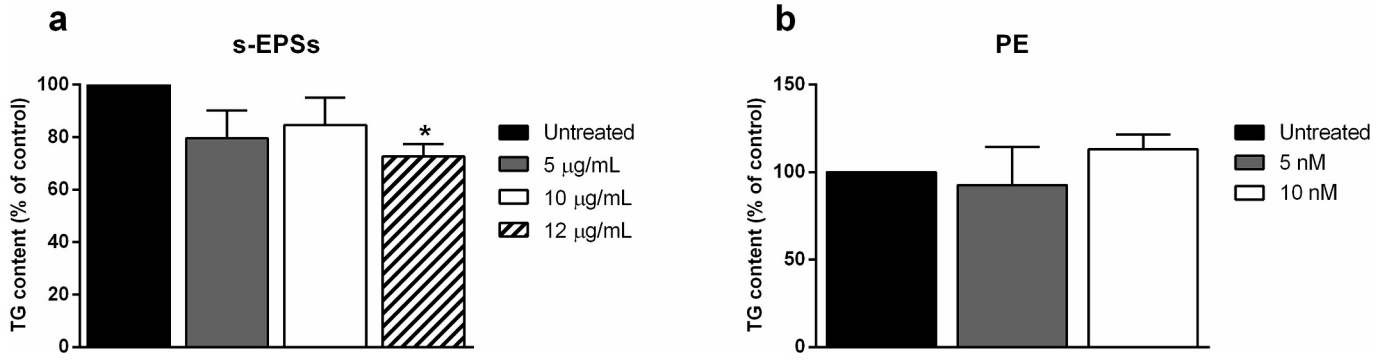

Fig. 5. Effects of s-EPSs and PE from *P. cruentum* on 3T3-L1 mature adipocyte triglyceride content. Triglyceride accumulation on mature adipocytes after 24 h treatment with (**a**) 5 μg/mL (dark grey bars), 10 μg/mL (white bars) or 12 μg/mL (white dashed bars) of s-EPSs; (**b**) 5 nM (grey bars) or 10 nM (white bars) of pure PE. Data are reported as the percentage of TG content with respect to cells differentiated in the absence of any molecule (black bars) and used as control. Results are reported as means ± S.D. of three independent experiments. * Indicates $p < 0.05$.

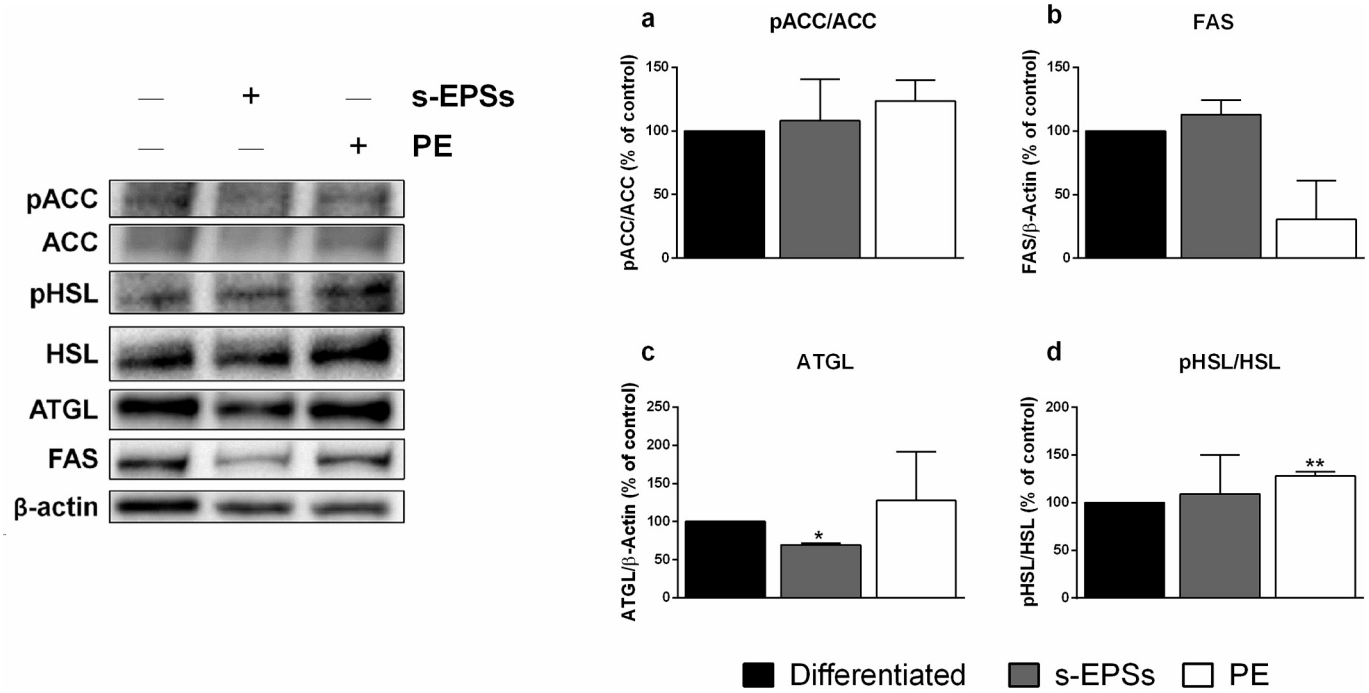

Fig. 6. Effect of s-EPSs and PE on the protein expression of *de novo* lipogenesis and lipolysis markers in 3T3-L1 mature adipocytes. 3T3-L1 mature adipocytes were incubated for 24 h with 12 μg/mL s-EPSs (grey bars) or 10 nM PE (white bars). Western blots show the phosphorylation levels of ACC (**a**) and HSL (**c**) with respect to their total amount; FAS and ATGL (**b, d**) are normalized with respect to β-actin. Black bars refer to cells differentiated in absence of any treatment and used as control. Data shown are the means ± S.D. of three independent experiments. * Indicates $p < 0.05$, ** indicates $p < 0.005$ with respect to control cells.

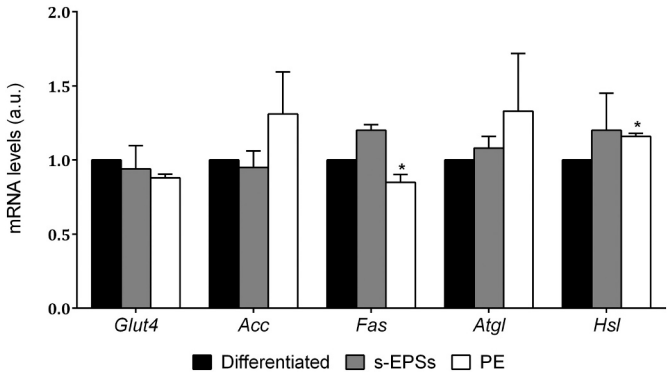

Fig. 7. Effects of s-EPSs and PE from *P. cruentum* on *de novo* lipogenesis and lipolysis-related genes. Relative mRNA levels of *Glut4*, *Acc*, *Fas*, *Atgl* and *Hsl* in mature 3T3-L1 after 24 h treatment with 12 μg/mL s-EPSs (grey bars) and 10 nM PE (white bars). Results are expressed as fold changes in threshold cycle (Ct) values compared to the controls (black bars) using the $2^{-\Delta\Delta Ct}$ method. Data shown are the means ± S.D. of three independent experiments. * Indicates $p < 0.05$.

which, in turn, negatively affects FAS synthesis but activates some inflammation-related markers (*e.g.* mTORC1 and PDE3) to turn on the *de novo* lipogenesis [44,45]. Once defined the experimental system, s-EPSs and PE activity were investigated after 18 h incubation. As shown in Fig. 9, s-EPSs partially prevented TG accumulation starting from 10 μg/mL (Fig. 9a, 45 %). In the case of PE treatment, the co-incubation with PA induced a significant increase in TG (Fig. 9b). Interestingly, s-EPSs treatment induced a significant increase in the pACC/ACC ratio, thus suggesting the prevalence of the enzyme in its phosphorylated-inactive form, along with a significant inhibition in FAS synthesis (Fig. 10a and Fig. 10b, grey bars), with respect to cells treated with PA. No alteration in pHSL/HSL ratio and ATGL expression was observed, indicating no activation of the lipolytic pathway. The negative results on TG accumulation upon PE incubation were corroborated by a reduction in pACC/ACC ratio, related to the active form of the enzyme, responsible for triglyceride synthesis (Fig. 10a, white bar). However, the significant decrease in FAS expression level (Fig. 10b, white bar) may suggest that no complete maturation of triglycerides occurs. Moreover, PE treatment did not modify ATGL expression but significantly reduced the pHSL/HSL ratio (Fig. 10c and Fig. 10d, white bars), suggesting no lipolysis activation.

4. Discussion

A sedentary lifestyle combined with external factors, such as a high-fat diet, can drastically increase lipid accumulation, which are stored in lipid droplets in the adipose tissue. The excessive number and the enlarged size of adipocytes can significantly alter their structure, leading to the development of skin-related disorders and, in worst cases, obesity [46]. It has been reported that oxidative stress is involved in many deleterious pathologies linked to an imbalance of lipid metabolism [47]. Indeed, oxidative stress enhances preadipocyte proliferation, adipocyte differentiation and growth [6] leading to adipocyte hypertrophy or hyperplasia, significantly affecting adipose tissue health and structure [48,49]. Consequently, cytokines and adipokines secreted by enlarged adipose cells induce insulin resistance, reduce lipolysis, and thus directly induce the translocation of fatty acids to the liver. These changes may represent the starting point for hepatic inflammatory states (also known as hepatic steatosis or nonalcoholic fatty liver disease (NAFLD)) that, in the worst-case scenario, can lead to the development of cirrhosis and hepatocellular carcinoma [4,50]. In this work, PE and s-EPSs obtained from the red microalga *P. cruentum* were tested as new tools for managing lipid metabolism in *in vitro* models of adipose tissue and hepatic steatosis. Both molecules were found to be fully biocompatible on 3T3-L1 cells, in line with the results previously reported by Liberti and colleagues on immortalized human keratinocytes (HaCaT) and immortalized murine fibroblasts (Balb/c-3T3) up to 72 h incubation [28]. Results obtained for s-EPSs highlighted their ability to reduce TG accumulation

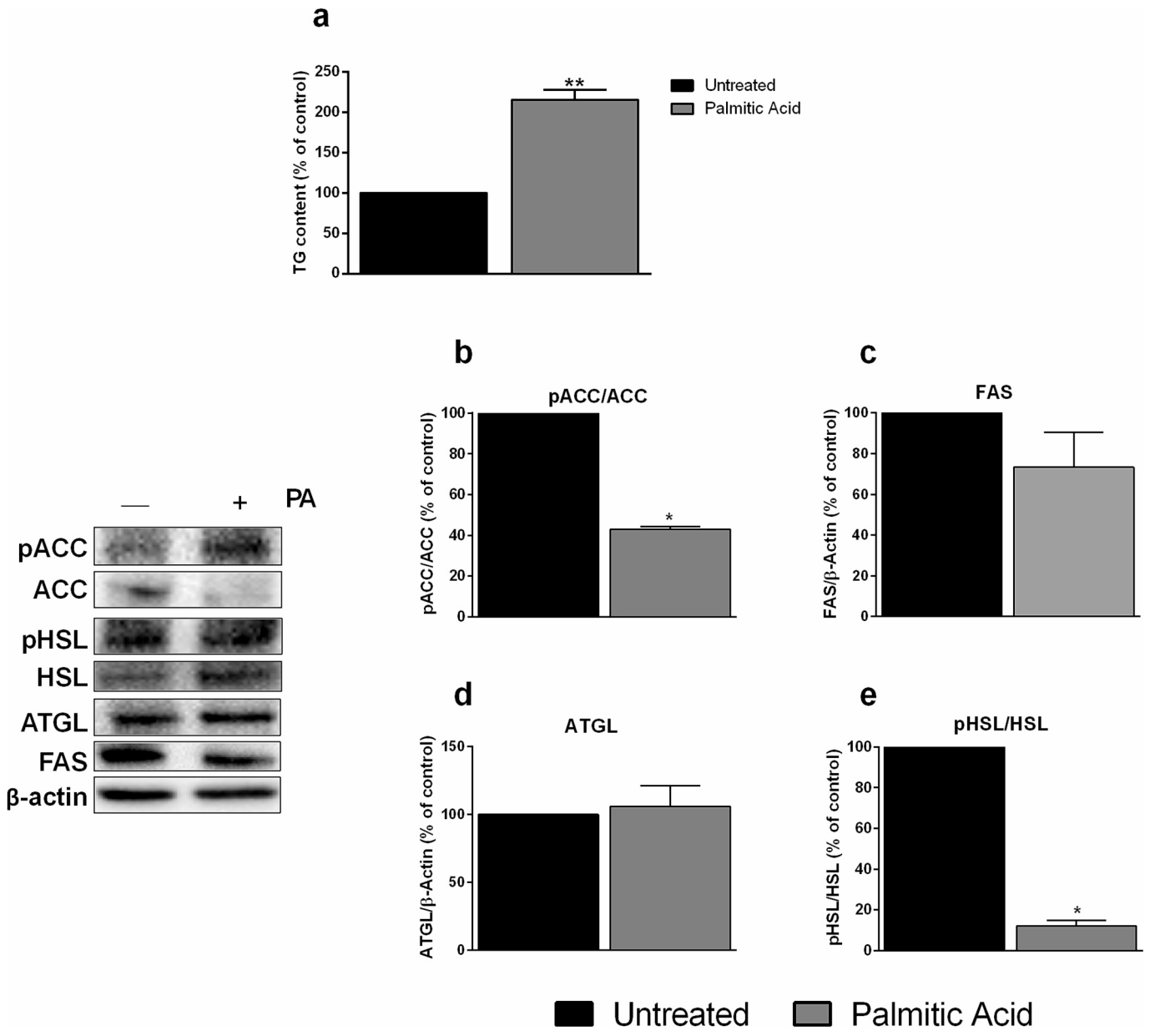

Fig. 8. Set-up of hepatic steatosis model on AML12 upon PA incubation. (**a**) Triglyceride accumulation on AML12 after 18 h incubation with palmitic acid (PA, dark grey bars); Western blots show the phosphorylation levels of ACC (**b**) and HSL (**e**) with respect to their total amount; FAS and ATGL (**c, d**) are normalized with respect to β-actin. Black bars refer to untreated cells used as control. Data shown are the means ± S.D. of three independent experiments. * Indicates $p < 0.05$; ** Indicates $p < 0.005$.

in 3T3-L1 pre-adipocytes in a dose-dependent manner, up to 90 % at the highest concentration tested (12 μg/mL). To date, only EPSs from probiotic or prebiotic bacterial strains were successfully used to inhibit TG accumulation. In particular, Lee reported a 60 % inhibition of TG content in pre-adipocytes upon treatment with 50 μg/mL of EPSs isolated from *Lactobacillus plantarum* [51], whereas Zhang and colleagues reached a 50 % inhibition with 10 μg/mL of EPSs from *Lactobacillus rhamnosus* GG [46]. Moreover, s-EPSs tested at 5 μg/mL were able to inhibit the gene and protein expression of three key transcriptional factors: c/EBPβ, PPARγ and adiponectin, thus affecting the differentiation process by modulating the early stages of the pathway. Coherent results have been reported also by Lee, who demonstrated that EPSs extracted from *Lactobacillus plantarum* inhibited adipocyte differentiation affecting c/EBPα and PPARγ gene and protein expression through AMPK signaling pathway [51]. Overall, despite the significant reduction in TG content on mature adipocytes, the present results do not fully clarify the small delipidating effect observed. Indeed, no significant modulation of *de novo* lipogenesis was observed, and a slight but significant inhibition of the lipolytic pathway (reduction in ATGL protein expression) was found. These contrasting results need a further investigation to understand if other enzymes involved in TG degradation or triacylglycerol mobilization might be upregulated or if lipophagy is involved, where the role played by ATGL is still controversial [52,53]. On the other hand, positive results were obtained in the hepatic steatosis model of AML12 treated with Palmitic Acid. In particular, even if s-EPSs did not activate the lipolytic pathway, they partially prevented TG accumulation. This could be explained by the inhibition of *de novo* lipogenesis, as indicated by ACC and FAS expression levels. The same results were reported by Zhang and colleagues who analyzed the protein expression in mice liver treated with EPSs obtained from *Lactobacillus rhamnosus* GG [46]. Despite studies on polysaccharides and exopolysaccharides from different sources, this is the first time in which s-EPSs

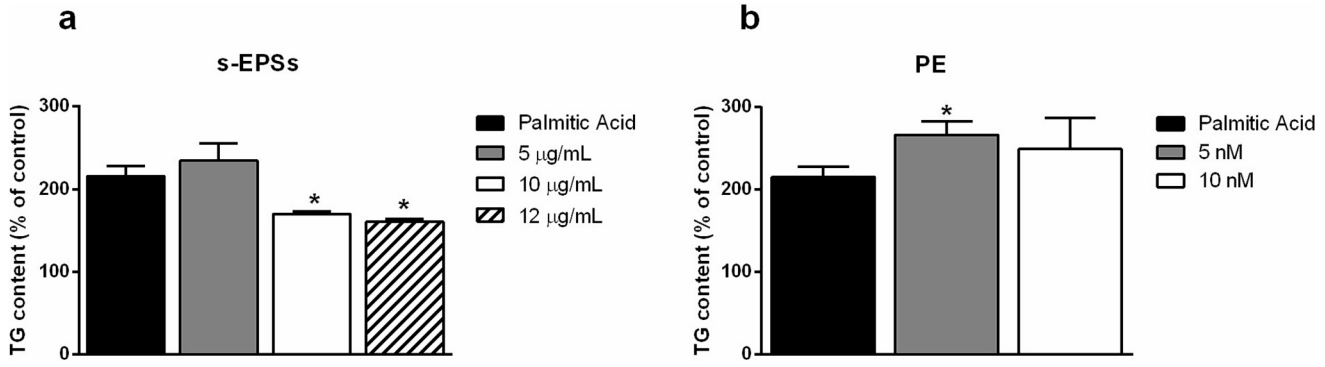

Fig. 9. Effects of s-EPSs and PE from *P. cruentum* on AML12 triglyceride accumulation. Triglyceride accumulation on AML12 after 18 h incubation with palmitic acid (PA, black bars) in presence or absence of s-EPSs (**a**) and PE (**b**). (**a**) 5 μg/mL (grey bars), 10 μg/mL (white bars) or 12 μg/mL (white dashed bars) of s-EPSs; (**b**) 5 nM (grey bars) or 10 nM (white bars) of pure PE. Data are reported as the percentage of TG content, with respect to PA-treated cells (black bars) used as control, normalized to the total protein content. Results are reported as means ± S.D. of three independent experiments. * $p < 0.05$ with respect to PA-treated cells.

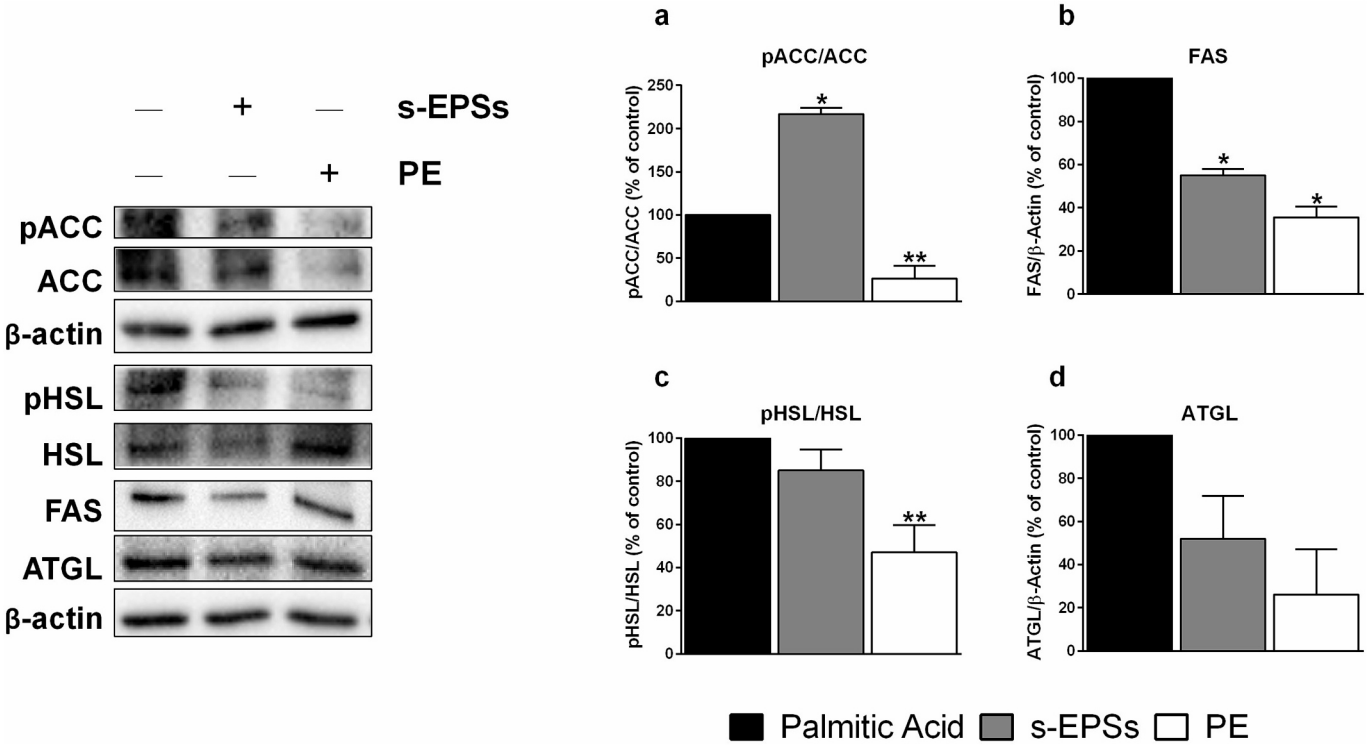

Fig. 10. Effect of s-EPSs and PE on AML12 lipid metabolism. AML12 hepatocytes were incubated for 18 h with 0.3 mM PA in the presence or absence of 10 μg/mL s-EPSs (grey bars) or 10 nM PE (white bars). Western blots show the phosphorylation levels of ACC (**a**) and HSL (**c**) with respect to their total amount; FAS and ATGL (**b, d**) are normalized with respect to β-actin. Black bars refer to cells treated with 0.3 mM PA alone and used as control. Data shown are the means ± S.D. of three independent experiments. * Indicates $p < 0.05$, ** indicates $p < 0.005$ with respect to PA-treated cells.

from microalgae have been tested for their ability to affect lipid metabolism in two cellular systems. Interestingly, the isolation of s-EPSs from microalgae do not require an extensive purification process, as it has been reported for those obtained from *Lactobacillus rhamnosus* GG [46]. Indeed, s-EPSs from microalgae require a simple ethanol precipitation to obtain pure polysaccharides, minimizing downstream purification steps and reducing processes costs. In addition, the presence of sulfur groups in s-EPSs may allow the formation of electrostatic bonds with surface receptors or intracellular proteins, influencing downstream signaling pathways [54,55].

The second analyzed molecule was Phycoerythrin, extracted from the wet biomass of *P. cruentum*. The purified protein was found to be fully biocompatible on 3T3-L1 cells and to induce a significant inhibition on TG production on 3T3-L1 pre-adipocytes, inhibiting the gene and protein expression of c/EBPβ, PPARγ and adiponectin. When mature adipocytes were treated with PE, no significant regulation of *de novo* lipogenesis protein markers was observed, even if a decreasing trend was observed, with the increase ACC inactive form and a decrease in the FAS protein and gene expression. Interestingly, PE incubation increased *Hsl* gene expression in its active form, thus boosting the activation of the last step of the lipolytic pathway. However, PE-induced lipogenesis at a molecular level, is not sufficient to reduce TG accumulation. In the case of AML12, the negative result on TG accumulation was corroborated by an increase in the active form of ACC, responsible for triglyceride synthesis. However, the significant decrease in FAS expression level may suggest that no complete maturation of triglycerides occurs. Moreover, lipolysis seemed not to be activated, as no alteration in ATGL expression was observed, whereas the pHSL/HSL ratio was significantly reduced.

The peculiar behavior observed for PE reflects its distinctive three-dimensional structure. As a globular protein of approximately 250 kDa, PE is unlikely to directly interact with transcription factors, but it may modulate intracellular molecular dynamics. Moreover, PE has been reported to regulate intracellular oxidative stress, a pathway strictly linked to lipid alteration [56–59]. Noteworthy, no evidence are present in literature about PE use on the proposed model system, with the exception of Qiang, who demonstrated the lipid-lowering activity in obese rats treated with a mixture of phycobiliproteins, fucoxanthin and krill oil [60].

Although the present study is pioneering, as PE and s-EPSs from a red marine microalga were used for the first time to study their activity on lipid metabolism, one should keep in mind that in-depth analyses are needed to unravel the interplay among the different involved pathways, such as lipophagy and oxidative stress. This study highlights the importance of defining the specific mechanism of action of each isolated molecule. Indeed, s-EPSs can inhibit adipocytes maturation and *de novo* lipogenesis on hepatic cells, whereas the interesting results obtained with PE on the inhibition of adipocytes maturation require more investigation, as the pro-fat effect induced on hepatic cells may represent a warning for possible therapeutic applications.

5. Conclusions

Lipid metabolism disorders share some common pathways, such oxidative stress impairment. However, each disorder is governed by specific key markers that define the onset of the pathology. This work highlights that antioxidant molecules can affect lipid metabolism disorders at different extents and that these pathologies are highly coordinated, with differences also at transcriptional and/or post-transcriptional level. Indeed, PE and s-EPSs from the red marine microalaga *P. cruentum*, despite the antioxidant activity, have a different mechanism of action, which can be due to their different physico-chemical characteristics. It is reasonable to speculate that the combination of different molecules from a single strain could enhance their individual potential, resulting in an innovative yet entirely natural therapeutic product.

CRediT authorship contribution statement

Enrica Giustino: Writing – original draft, Validation, Methodology, Investigation, Formal analysis, Data curation. **Paola Imbimbo:** Writing – review & editing, Supervision, Investigation, Formal analysis, Conceptualization. **Jenifer Trepiana:** Writing – review & editing, Supervision. **Maria P. Portillo:** Writing – review & editing, Supervision, Resources, Conceptualization. **Daria Maria Monti:** Writing – review & editing, Supervision, Resources, Project administration, Conceptualization.

Declaration of competing interest

The authors declare that they have no competing financial interests or personal relationships that could have appeared to influence the work reported in this paper.

Acknowledgements

The authors acknowledge the financial support provided by the Government of the Basque Country (IT1482-22) for the work of Jenifer Trepiana.

Data availability

Data will be made available on request.

References

[1] T.R. Klran, O. Otlu, A.B. Karabulut, Oxidative stress and antioxidants in health and disease, J. Lab. Med. 47 (2023) 1–11, https://doi.org/10.1515/labmed-2022-0108.
[2] E. Birben, U. Sahiner, C. Sackesen, S. Erzurum, O. Kalayci, Oxidative stress and antioxidant defense mechanism in, WAO J. 22 (2012) 9–19.
[3] E. Čolak, D. Pap, The role of oxidative stress in the development of obesity and obesity-related metabolic disorders, J. Med. Biochem. 40 (2021) 1–9, https://doi.org/10.5937/jomb0-24652.
[4] V.J. Clemente-Suárez, A.I. Beltrán-Velasco, L. Redondo-Flórez, A. Martín-Rodríguez, J.F. Tornero-Aguilera, Global impacts of Western diet and its effects on metabolism and health: a narrative review, Nutrients 15 (2023), https://doi.org/10.3390/nu15122749.
[5] S.K. Masenga, L.S. Kabwe, M. Chakulya, A. Kirabo, Mechanisms of oxidative stress in metabolic syndrome, Int. J. Mol. Sci. 24 (2023), https://doi.org/10.3390/ijms24097898.
[6] C. Rives, A. Fougerat, S. Ellero-Simatos, N. Loiseau, H. Guillou, L. Gamet-Payrastre, W. Wahli, Oxidative stress in NAFLD: role of nutrients and food contaminants, Biomolecules 10 (2020), https://doi.org/10.3390/biom10121702.
[7] I. Pérez-Torres, V. Castrejón-Téllez, M.E. Soto, M.E. Rubio-Ruiz, L. Manzano-Pech, V. Guarner-Lans, Oxidative stress, plant natural antioxidants, and obesity, Int. J. Mol. Sci. 22 (2021), https://doi.org/10.3390/ijms22041786.
[8] K. Il Oh, E. Lim, L.P. Uprety, J. Jeong, H. Jeong, E. Park, S.Y. Jeong, Anti-adipogenic and anti-obesity effects of morroniside *in vitro* and *in vivo*, Biomed. Pharmacother. 176 (2024) 116762, https://doi.org/10.1016/j.biopha.2024.116762.
[9] A. Geier, D. Tiniakos, H. Denk, M. Trauner, From the origin of NASH to the future of metabolic fatty liver disease, Gut 70 (2021) 1570–LP-1579, https://doi.org/10.1136/gutjnl-2020-323202.
[10] S. Murag, A. Ahmed, D. Kim, Recent epidemiology of nonalcoholic fatty liver disease, Gut Liver 15 (2021) 206–216, https://doi.org/10.5009/gnl20127.
[11] F. Pérez-Aguilar, Etiopathogenesis of non-alcoholic steatohepatitis, Gastroenterol. Hepatol. 28 (2005) 396–406, https://doi.org/10.1157/13077761.
[12] L. Rong, J. Zou, W. Ran, X. Qi, Y. Chen, H. Cui, J. Guo, Advancements in the treatment of non-alcoholic fatty liver disease (NAFLD), Front. Endocrinol. (Lausanne) 13 (2023) 1–18, https://doi.org/10.3389/fendo.2022.1087260.
[13] H. Goshtasbi, Y.B. Okolodkov, A. Movafeghi, S. Awale, A. Safary, J. Barar, Y. Omidi, Harnessing microalgae as sustainable cellular factories for biopharmaceutical production, Algal Res. 74 (2023) 103237, https://doi.org/10.1016/j.algal.2023.103237.
[14] P. Mapelli-Brahm, P. Gómez-Villegas, M.L. Gonda, A. León-Vaz, R. León, J. Mildenberger, C. Rebours, V. Saravia, S. Vero, E. Vila, A.J. Meléndez-Martínez, Microalgae, seaweeds and aquatic Bacteria, Archaea, and yeasts: sources of carotenoids with potential antioxidant and anti-inflammatory health-promoting actions in the sustainability era, Mar. Drugs 21 (2023), https://doi.org/10.3390/md21060340.
[15] K.R. LeFort, W. Rungratanawanich, B.J. Song, Contributing roles of mitochondrial dysfunction and hepatocyte apoptosis in liver diseases through oxidative stress, post-translational modifications, inflammation, and intestinal barrier dysfunction, Cell. Mol. Life Sci. 81 (2024), https://doi.org/10.1007/s00018-023-05061-7.
[16] M.J. Kiki, Biopigments of microbial origin and their application in the cosmetic industry, Cosmetics 10 (2023), https://doi.org/10.3390/cosmetics10020047.
[17] J.V. Barreto, L.M. Casanova, A.N. Junior, M.C. Reis-Mansur, A.B. Vermelho, Microbial pigments: major groups and industrial applications, Microorganisms 11 (2023), https://doi.org/10.3390/microorganisms11122920.
[18] K.D. Athiyappan, W. Routray, B. Paramasivan, Phycocyanin from *Spirulina*: a comprehensive review on cultivation, extraction, purification, and its application in food and allied industries, Food Humanit. 2 (2024) 100235, https://doi.org/10.1016/j.foohum.2024.100235.
[19] T.J. Ashaolu, The powerful phycobiliproteins-phycocyanin and phycoerythrin: pleiotropic applications and biofunctional uses, Algal Res. 82 (2024) 103636, https://doi.org/10.1016/j.algal.2024.103636.
[20] G. Nieto, L. Martínez-Zamora, R. Peñalver, F. Marín-Iniesta, A. Taboada-Rodríguez, A. López-Gómez, G.B. Martínez-Hernández, Applications of plant bioactive compounds as replacers of synthetic additives in the food industry, Foods 13 (2024), https://doi.org/10.3390/foods13010047.
[21] N. Coulombier, T. Jauffrais, N. Lebouvier, Antioxidant compounds from microalgae: a review, Mar. Drugs 19 (2021), https://doi.org/10.3390/md19100549.
[22] R. George, J.A. John, Phycoerythrin as a potential natural colourant: a mini review, Int. J. Food Sci. Technol. 58 (2023) 513–519, https://doi.org/10.1111/ijfs.16229.
[23] W. Levasseur, P. Perré, V. Pozzobon, A review of high value-added molecules production by microalgae in light of the classification, Biotechnol. Adv. 41 (2020) 107545, https://doi.org/10.1016/j.biotechadv.2020.107545.
[24] J. Fan, J. Zhu, H. Zhu, Y. Zhang, H. Xu, Potential therapeutic target for polysaccharide inhibition of colon cancer progression, Front. Med. 10 (2024), https://doi.org/10.3389/fmed.2023.1325491.
[25] D. Zhuang, N. He, K.S. Khoo, E.P. Ng, K.W. Chew, T.C. Ling, Application progress of bioactive compounds in microalgae on pharmaceutical and cosmetics, Chemosphere 291 (2022) 132932, https://doi.org/10.1016/j.chemosphere.2021.132932.
[26] W. Guo, S. Zhu, S. Li, Y. Feng, H. Wu, M. Zeng, Microalgae polysaccharides ameliorates obesity in association with modulation of lipid metabolism and gut microbiota in high-fat-diet fed C57BL/6 mice, Int. J. Biol. Macromol. 182 (2021) 1371–1383, https://doi.org/10.1016/j.ijbiomac.2021.05.067.

[27] D. Liberti, P. Imbimbo, E. Giustino, L. D'elia, G. Ferraro, A. Casillo, A. Illiano, G. Pinto, M.C. Di Meo, G. Alvarez-Rivera, M.M. Corsaro, A. Amoresano, A. Zarrelli, E. Ibáñez, A. Merlino, D.M. Monti, Inside out *Porphyridium cruentum*: beyond the conventional biorefinery concept, ACS Sustain. Chem. Eng. (2022), https://doi.org/10.1021/acssuschemeng.2c05869.
[28] D. Liberti, P. Imbimbo, E. Giustino, L. D'Elia, M. Silva, L. Barreira, D.M. Monti, Shedding light on the hidden benefit of *Porphyridium cruentum* culture, Antioxidants 12 (2023) 1–12, https://doi.org/10.3390/antiox12020337.
[29] P. Imbimbo, E. Giustino, A. Ferrara, G. Alvarez, R. Hassan, A. Elena, M. Chiara, D. Meo, A. Zarrelli, D. Maria, Unveiling the potential of *Pseudococcomyxa simplex* : a stepwise extraction for cosmetic applications, Appl. Microbiol. Biotechnol. (2024), https://doi.org/10.1007/s00253-024-13229-9.
[30] M. Singh, T. Thrimawithana, R. Shukla, C.S. Brennan, B. Adhikari, Impact of phenolic extracts and potassium hydroxycitrate of Hibiscus sabdariffa on adipogenesis: a cellular study, Int. J. Food Sci. Technol. 58 (2023) 1204–1218, https://doi.org/10.1111/ijfs.16269.
[31] M. González-Arceo, J. Trepiana, L. Aguirre, J. Ibarruri, M. Martínez-Sanz, M. Cebrián, I. Recio, M.P. Portillo, S. Gómez-Zorita, Anti-Steatotic effects of Chlorella vulgaris, Nannochloropsis gaditana and Gracilaria vermiculophylla algae extracts in AML-12 hepatocytes, Nutrients 15 (2023), https://doi.org/10.3390/nu15081960.
[32] P. Beaumont, S. Amintas, S. Krisa, A. Courtois, T. Richard, I. Eseberri, M.P. Portillo, Glucuronide metabolites of trans-ε-viniferin decrease triglycerides accumulation in an in vitro model of hepatic steatosis, J. Physiol. Biochem. (2024) 2–13, https://doi.org/10.1007/s13105-024-01035-w.
[33] M.M. Bradford, A rapid and sensitive method for the quantitation of microgram quantities of protein utilizing the principle of protein-dye binding, Anal. Biochem. 72 (1976) 248–254, https://doi.org/10.1016/0003-2697(76)90527-3.
[34] P.K. Smith, R.I. Krohn, G.T. Hermanson, A.K. Mallia, F.H. Gartner, M. D. Provenzano, E.K. Fujimoto, N.M. Goeke, B.J. Olson, D.C. Klenk, Measurement of protein using bicinchoninic acid, Anal. Biochem. 150 (1985) 76–85, https://doi.org/10.1016/0003-2697(85)90442-7.
[35] I. Eseberri, J. Miranda, A. Lasa, A. Mosqueda-Solís, S. González-Manzano, C. Santos-Buelga, M.P. Portillo, Effects of quercetin metabolites on triglyceride metabolism of 3T3-L1 preadipocytes and mature adipocytes, Int. J. Mol. Sci. 20 (2019), https://doi.org/10.3390/ijms20020264.
[36] K.J. Livak, T.D. Schmittgen, Analysis of relative gene expression data using real-time quantitative PCR and the 2(-Delta Delta C(T)) method, Methods 25 (2001) 402–408, https://doi.org/10.1006/meth.2001.1262.
[37] B. Fernández-Rojas, J. Hernández-Juárez, J. Pedraza-Chaverri, Nutraceutical properties of phycocyanin, J. Funct. Foods 11 (2014) 375–392, https://doi.org/10.1016/j.jff.2014.10.011.
[38] C. Iacobini, M. Vitale, J. Haxhi, S. Menini, G. Pugliese, Impaired remodeling of white adipose tissue in obesity and aging: from defective Adipogenesis to adipose organ dysfunction, Cells 13 (2024), https://doi.org/10.3390/cells13090763.
[39] W.Y. Hsiao, D.A. Guertin, De novo lipogenesis as a source of second messengers in adipocytes, Curr. Diab. Rep. 19 (2019), https://doi.org/10.1007/s11892-019-1264-9.
[40] Y. Li, Z. Li, D.A. Ngandiri, M. Llerins Perez, A. Wolf, Y. Wang, The molecular brakes of adipose tissue lipolysis, Front. Physiol. 13 (2022) 1–19, https://doi.org/10.3389/fphys.2022.826314.
[41] J. Li, C. Li, X. Wu, Y. Dong, Y. Li, X. Jiao, J. Li, L. Han, M. Wang, Protocatechuic acid suppresses lipid uptake and synthesis through the PPARγ pathway in high-fat diet-induced NAFLD mice, J. Agric. Food Chem. (2025), https://doi.org/10.1021/acs.jafc.4c01354.
[42] M.V. Chakravarthy, Z. Pan, Y. Zhu, K. Tordjman, J.G. Schneider, T. Coleman, J. Turk, C.F. Semenkovich, "New" hepatic fat activates PPARα to maintain glucose, lipid, and cholesterol homeostasis, Cell Metab. 1 (2005) 309–322, https://doi.org/10.1016/j.cmet.2005.04.002.
[43] D.H. Ipsen, J. Lykkesfeldt, P. Tveden-Nyborg, Molecular mechanisms of hepatic lipid accumulation in non-alcoholic fatty liver disease, Cell. Mol. Life Sci. 75 (2018) 3313–3327, https://doi.org/10.1007/s00018-018-2860-6.
[44] C. Dorn, M.-O. Riener, G. Kirovski, M. Saugspier, K. Steib, T.S. Weiss, E. Gäbele, G. Kristiansen, A. Hartmann, C. Hellerbrand, Expression of fatty acid synthase in nonalcoholic fatty liver disease, Int. J. Clin. Exp. Pathol. 3 (2010) 505–514.
[45] Z. Zhu, X. Zhang, Q. Pan, L. Zhang, J. Chai, In-depth analysis of de novo lipogenesis in non-alcoholic fatty liver disease: mechanism and pharmacological interventions, Liver Res. 7 (2023) 285–295, https://doi.org/10.1016/j.livres.2023.11.003.
[46] Z. Zhang, Z. Zhou, Y. Li, L. Zhou, Q. Ding, L. Xu, Isolated exopolysaccharides from lactobacillus rhamnosus GG alleviated adipogenesis mediated by TLR2 in mice, Sci. Rep. 6 (2016) 1–14, https://doi.org/10.1038/srep36083.
[47] D.K. Sahoo, R.M. Heilmann, B. Paital, A. Patel, V.K. Yadav, D. Wong, A.E. Jergens, Oxidative stress, hormones, and effects of natural antioxidants on intestinal inflammation in inflammatory bowel disease, Front. Endocrinol. (Lausanne) 14 (2023), https://doi.org/10.3389/fendo.2023.1217165.
[48] V. Rani, G. Deep, R.K. Singh, K. Palle, U.C.S. Yadav, Oxidative stress and metabolic disorders: pathogenesis and therapeutic strategies, Life Sci. 148 (2016) 183–193, https://doi.org/10.1016/j.lfs.2016.02.002.
[49] G. Grosso, D. Laudisio, E. Frias-Toral, L. Barrea, G. Muscogiuri, S. Savastano, A. Colao, Anti-inflammatory nutrients and obesity-associated metabolic-inflammation: state of the art and future direction, Nutrients 14 (2022), https://doi.org/10.3390/nu14061137.
[50] T.V. Rohm, D.T. Meier, J.M. Olefsky, M.Y. Donath, Inflammation in obesity, diabetes, and related disorders, Immunity 55 (2022) 31–55, https://doi.org/10.1016/j.immuni.2021.12.013.
[51] J. Lee, S. Park, N. Oh, J. Park, M. Kwon, J. Seo, S. Roh, Oral intake of lactobacillus plantarum L-14 extract alleviates TLR2- and AMPK-mediated obesity-associated disorders in high-fat-diet-induced obese C57BL/6J mice, Cell Prolif. 54 (2021) 1–14, https://doi.org/10.1111/cpr.13039.
[52] S.L. Han, Y.C. Qian, S.M. Limbu, J. Wang, L.Q. Chen, M.L. Zhang, Z.Y. Du, Lipolysis and lipophagy play individual and interactive roles in regulating triacylglycerol and cholesterol homeostasis and mitochondrial form in zebrafish, Biochim. Biophys. Acta Mol. Cell Biol. Lipids 1866 (2021) 158988, https://doi.org/10.1016/j.bbalip.2021.158988.
[53] R. Li, G. Li, Y. Hai, T. Li, Y. Bian, T. Ma, The effect of aerobic exercise on the lipophagy of adipose tissue in obese male mice, Chem. Phys. Lipids 247 (2022) 105225, https://doi.org/10.1016/j.chemphyslip.2022.105225.
[54] B. Jegadeshwari, R. Rajaram, A critical review on pharmacological properties of sulfated polysaccharides from marine macroalgae, Carbohydr. Polym. 344 (2024) 122488, https://doi.org/10.1016/j.carbpol.2024.122488.
[55] Q. Chen, M. Zhang, Y. Liu, W. Liu, C. Peng, L. Zheng, Sulfated polysaccharides with anticoagulant potential: a review focusing on structure-activity relationship and action mechanism, Chem. Biodivers. 21 (2024) e202400152, https://doi.org/10.1002/cbdv.202400152.
[56] Y. Wen, S. Shan, F. Ye, W. Liao, X. Wu, W. Chen, C. Zhao, Prospects of phycoerythrin: structural features, antioxidation and applications in food, Food Chem. 463 (2025) 141425, https://doi.org/10.1016/j.foodchem.2024.141425.
[57] V. Kumar, R.R. Sonani, M. Sharma, G.D. Gupta, D. Madamwar, Crystal structure analysis of C-phycoerythrin from marine cyanobacterium Phormidium sp. A09DM, Photosynth. Res. 129 (2016) 17–28, https://doi.org/10.1007/s11120-016-0259-5.
[58] R.R. Sonani, R.P. Rastogi, N.K. Singh, J. Thadani, P.J. Patel, J. Kumar, A.K. Tiwari, R.V. Devkar, D. Madamwar, Phycoerythrin averts intracellular ROS generation and physiological functional decline in eukaryotes under oxidative stress, Protoplasma 254 (2017) 849–862, https://doi.org/10.1007/s00709-016-0996-5.
[59] E. Giustino, P. Imbimbo, J. Trepiana, M.P. Portillo, D.M. Monti, Unlocking the Antiadipogenic potential of carotenoids from Galdieria phlegrea, BioFactors 51 (2025) 1–13, https://doi.org/10.1002/biof.70027.
[60] X. Qiang, C. Guo, W. Gu, Y. Song, Y. Zhang, X. Gong, L. Wang, G. Wang, The complex of Phycobiliproteins, Fucoxanthin, and krill oil ameliorates obesity through modulation of lipid metabolism and antioxidants in obese rats, Nutrients 14 (2022), https://doi.org/10.3390/nu14224815.
[61] J. Vignaud, C. Loiseau, J. Hérault, C. Mayer, M. Côme, I. Martin, L. Ulmann, Microalgae Produce Antioxidant Molecules with Potential Preventive Effects on Mitochondrial Functions and Skeletal Muscular Oxidative Stress, Antioxidants 12 (5) (2023) 1050, https://doi.org/10.3390/antiox12051050.